Investigation of Creep-Fatigue Lifetime in Solar Photovoltaic Module Interconnections

Alireza Eslami Majd[1], Nduka Nnamdi Ekere[2], Armin Rahmati Darvazi[3], Ali Amini Sedehi[4] and Fideline Tchuenbou-Magaia[1]

[1]Faculty of Science and Engineering, University of Wolverhampton, Wolverhampton (UK)
[2]Faculty of Engineering and Technology, Liverpool John Moores University, Liverpool (UK)
[3]Faculty of Technology and Engineering, University of Guilan, Rasht (Iran)
[4]Faculty of Mechanical Engineering, University of Kashan, Kashan (Iran)

Abstract

The growing demand for utilization of solar photovoltaic (PV) module puts increased pressure on manufacturers to improve the reliability of PV modules for meeting their lifetime warranty. The PV module interconnection which is one of the key components of the module is reported to account for about 40% of the failure of the module. In this study, Finite Element Analysis using ABAQUS software was used to investigate the creep-fatigue behavior of the solder joints for convectional PV module interconnection with different dimensions. The exponent factor of the Coffin–Manson–Arrhenius approach for estimating the creep-fatigue life of the PV module interconnections was determined to be -1.8 and was used to predict the solder joint's creep-fatigue life under thermal cycling operating conditions. Our results also suggest that optimal dimensions for higher creep-fatigue life and PV interconnection reliability are 20µm solder thickness, 40µm-50µm silver-pad thickness, 150µm copper thickness and 1mm ribbon width.

Keyword: PV Module Interconnection, Reliability, Creep-Fatigue, Life Time.

1. Introduction

As the PV Solar module technology is being developed to play a more significant role in the replacement of fossil fuel sources with renewable energy sources, the challenge to improve the reliability of the PV modules is getting more attention. According to a recent IRENA (International Renewable Energy Agency) report (IRENA 2019), solar PV will become the second-largest power generation source by 2050 (just behind wind power) and will be the catalyst for the transformation of the global electricity sector, generating some 25% of total electricity needs globally. In order to grow the global share of electricity generation of Solar PV from the current 3% (IEA, 2020) to the projected 25% by 2050, there is an urgent need for improving the reliability of PV modules, which have been reported to fail due to adverse operating conditions such as thermal cycling, damp heat and UV exposure. For example, thermal cycling can cause PV module interconnection solder joint failures and cracks in solar cells (Ogbomo, et al., 2018).

Solar PV module manufacturers are also keen to achieve higher reliability products in order to match their offer of power output warranties of 25 years (with early and premature failures covered by the warranty and the free replacement of the solar PV module). Study of the potential failure modes of PV module have shown that one of the major PV module's reliability challenges is the failure of the solder joint materials used for connecting the ribbon to the cell. This is because the daily power-up and shut-down and the associated heating and cooling down of the PV module results in thermal cycling and ageing of the PV module. Consequently, the solder joints used for the PV module interconnection can experience very high stress and strain levels due to the coefficient of the thermal expansion (CTE) mismatch between the adjacent materials (Itoh, et al., 2014). The induced stress and strain in the solder joints result in high levels of energy accumulation that can significantly reduce the creep-fatigue life of the interconnection and the long-term reliability of the PV module (Ogbomo, et al., 2018). Also, during the high temperature manufacturing processes of the PV module (e.g. EVA lamination), the CTE mismatch between the materials can cause the micro-cracks in the solder joints, which can then result in a premature interconnection failure (Majd, Ekere, 2020a).

doi:10.18086/eurosun.2022.07.03 Available at http://proceedings.ises.org

The models for estimation of the fatigue life of solder joints can be sub-divided into three categories, namely: stress-based, strain-based and energy-based approaches. According to the stress-based approach, fatigue failure occurs when the accumulated stress reaches a trigger threshold (Li, et al., 2017; Han, Han, 2014). The strain-based approach is the most widely reported method in the literature for the computational study of creep-fatigue behavior of the solder joints. For strain-based fatigue models, the strain is composed of the elastic strain, plastic strain, creep strain components, which are not easily distinguishable (Knetch, Fox, 1990). The Coffin-Manson model and the Total Strain model are two of the most popular strain-based models used for the prediction of the thermal fatigue life of materials (Li, et al., 2017; Lee, et al., 2000). The Coffin-Manson model uses the plastic strain amplitude over a cycle to estimate the number of cycles to failure. Several modifications of the Coffin-Manson model have been used for the prediction of the fatigue life of materials in specific conditions (Chen, et al., 2017). For example, Yunxia Chen et al. used the modified Coffin-Manson equation to introduce a coupling damage model considered low-cycle fatigue and creep (Chen, et al., 2021). It was also found that for strain levels less than 1%, the Coffin-Manson model cannot accurately estimate the creep-fatigue life, and hence is not recommended, as the strain is mostly composed of creep and elastic strains rather than plastic strain (Hund, Burchett, 1991). The total strain model was introduced as a modified form of the Coffin–Manson model to incorporate both the elastic and plastic strain terms (Lee, et al., 2000; Yao, et al. 2017).

In terms of the energy-based models used for predicting the creep-fatigue life of materials, the Morrow Energy Density model (Andersson et al., 2006; Zhu et al., 2014), is one of the most widely used methods. In this approach, the plastic strain energy density is used instead of the plastic strain values. The advantage of this method is that it incorporates the effects of both plastic strain and plastic stress on the cumulative energy. In the Morrow Energy Density model, the number of cycles to failure (N_f) is a function of the plastic strain energy density, which is obtained from the hysteresis stress-strain loops for each cycle. In another study, Akay et al. developed the model for predicting the creep-fatigue life based on the total strain energy, rather than the plastic strain energy density (Akay, et al., 2003). The stress–strain hysteresis energy is also important for predicting the fatigue failure life (Steinhorst, et al., 2013)). For example, Darveaux proposed a fatigue model with consideration of the accumulated stress–strain hysteresis energy in the material to derive the equation for the crack initiation cycle number and crack propagation rate (Darveaux, 2002).

The strain and the energy terms used in the models discussed above for the estimation of the fatigue life of materials can be found by using the analytical constitutive models of creep behavior. Examples of the constitutive models used for the prediction of the creep fatigue life of materials include the following: (a). Garofalo or Hyperbolic Sine (Syed, 2004; Depiver, et al., 2021), (b). Anand (Baber, Guven, 2017; Cho, et al., 2018), (c). Johnson-Cook (Halounai, et al., 2020) and (d). Power Law (Zhang, et al., 2008; Ma, 2009).

In this study, the Hyperbolic-Sine creep model in ABAQUS software was used to study the creep behavior of the solder joints for PV module interconnection with different dimensions. The total dissipated energy extracted from FEM simulation was used to find the number of cycles to failure for the solder joints using reliability formulation. For this reliability, a Coffin–Manson–Arrhenius exponent factor was found by comparing different thermal cycling conditions. Then this factor was used to determine the creep-fatigue life of the solder joints in PV module interconnection under arbitrary thermal cycling conditions.

2. Methodology

2.1. Creep Investigation Model

Previous studies on the failure of solder materials showed that they exhibit elastic, bilinear kinematic hardening plastic behavior after yielding (Che, Pang, 2004). The Hyperbolic-Sine creep model is perhaps, one of the most widely reported in the literature for investigating the effect of temperature and strain rate on the elastic plastic creep behavior of materials. Amalu, et al. (2016) compared different set of creep parameter values of the lead-free solder joints to select a suitable constitutive model based on the Hyperbolic-Sine creep model to predict the accurate creep parameters (Amalu, Ekere, 2016). Equation 1 shows the formula for the Hyperbolic-Sine creep model.

$$\dot{\varepsilon}_{cr} = A\left(\sin \mathrm{h}(\beta\sigma)\right)^{n} exp\left(-\frac{Q}{RT}\right) \qquad \text{(eq. 1)}$$

where $\dot{\varepsilon}_{cr}$ is the scalar creep strain rate, A is Boltzmann's constant, β and n are constants, σ is the von-mises effective stress, Q is activation energy, R is gas constant and T is the absolute temperature. The values of the parameters in the hyperbolic sine creep equation for popular SAC (Tin, Silver, Copper) solder alloys (e.g. Sn3.8Ag0.7Cu, Sn3.5Ag0.75Cu and Sn3.5Ag0.5Cu) have been found to be as follows: β is 0.02447 1/MPa, n is 6.41, R is 8.314 J·Mol−1·K−1 and $\frac{Q}{R}$ is 6500 (Schubert, et al., 2003).

2.2. FEM Simulation

In this study, the FEM simulation for different dimensions of the conventional PV module interconnection ribbon was performed in ABAQUS 2019 and the Hyperbolic-Sine creep model was applied to the solder joint material. Tab. 1 presents the mechanical properties of the material used for the FEM simulation. As the plastic behavior of the solder joint material is considered temperature dependent, the values for the coefficient of thermal expansion of the materials, the Young's Modulus and the plastic stress for the solder joint material used for investigating the effect of temperature on the elastic plastic creep behavior of materials are given in Tab. 2.

Tab. 1: Mechanical Properties of material used in the FEM simulation of PV module interconnection (Majd, Ekere, 2020a).

	IMC-Copper (Cu5Sn6)	IMC-Silver (Ag3Sn)	Solder (SAC)	Silver	Al	Copper	EVA	Silicon	Tedlar	Glass
Elastic Modulus (GPa)	110	79	See Tab. 2	69	68.3	121	11	130	2.138	73.0
Poisson's Ratio	0.3	0.3	0.35	0.365	0.34	0.34	0.499	0.28	0.4	0.235
Yield Stress (MPa)	-	-	-	43	85	121	12	170	41	-
Thermal Expansion Coefficient (ppm/K)	See Tab. 2	See Tab. 2	See Tab. 2	See Tab. 2	See Tab. 2	See Tab. 2	270	See Tab. 2	78	8.0
Plastic Stress (MPa) @ Strain	-	-	See Tab. 2	43@0.001 120@0.04	85@0.001 100@0.12	121@0.001 217@0.01 234@0.02 248@0.04	-	-	41@0.00 55@0.9	-

Tab. 2: Temperature dependency of the material properties used in the FEM simulation (Majd, Ekere, 2020a).

Temp. (°C)	Interpolated data for the Coefficient of Thermal Expansion (ppm/K)							Young's Modulus (GPa)	Yield Stress (MPa)	Plastic Stress (MPa) at 0.065 Strain
	Copper	Silver	Al	Silicon	IMC-Copper (Cu5Sn6)	IMC-Silver (Ag3Sn)	Solder	Solder (SAC)		
0	16.22	18.67	22.50	2.35	17.7	19	21.3	49	71	145
30	16.60	18.98	23.29	2.63	18	19.4	21.81	46.9	52	131
60	16.91	19.20	23.85	2.87	18.3	19.8	22.32	44.8	16	110
90	17.22	19.42	24.41	3.04	18.6	20.3	22.83	42.7	-	-
120	17.53	19.65	24.97	3.20	19	20.7	23.34	40.6	-	-
150	17.76	19.91	25.40	3.36	19.8	21.1	23.85	38.5	-	-

To increase the computational solution speed, the 2D plane-strain elements were used since the geometry of the models have a high ratio of the interconnection length to the other dimensions of model. The symmetry boundary condition was applied to the mid-point of the interconnection section and bottom-end of the Tedlar material was closed. Fig. 1 is a schematic view of the cross section of the conventional PV module interconnection showing the applied boundary conditions and the solder joint mesh design used for the FEM simulation in ABAQUS. The models were subjected to a homogenous thermal cycling load, with time history in accordance with the IEC 61215-2:2016 standard (the temperature of cycle uniformly changes between the

minimum temperature (-40°C) and maximum temperature (85°C) with the rate 100°C/hr during 15 minutes and with 10 minutes dwell time) (International Electrotechnical Commission, 2016). In this study, the thickness of the materials used for the models (namely, aluminum, silicon cell, EVA, glass and Tedlar layers), were assumed to be 25µm, 200µm, 460µm, 3mm and 190µm, respectively. Also, the thickness of the IMC (intermetallic compound) layer in the boundaries of the solder joint with the copper and silver-pad materials is considered to be 4 µm. The interconnection width and the thickness of other component parts including silver-pad, copper, and the solder joints are then varied to investigate the effect of interconnection design on the creep-fatigue response.

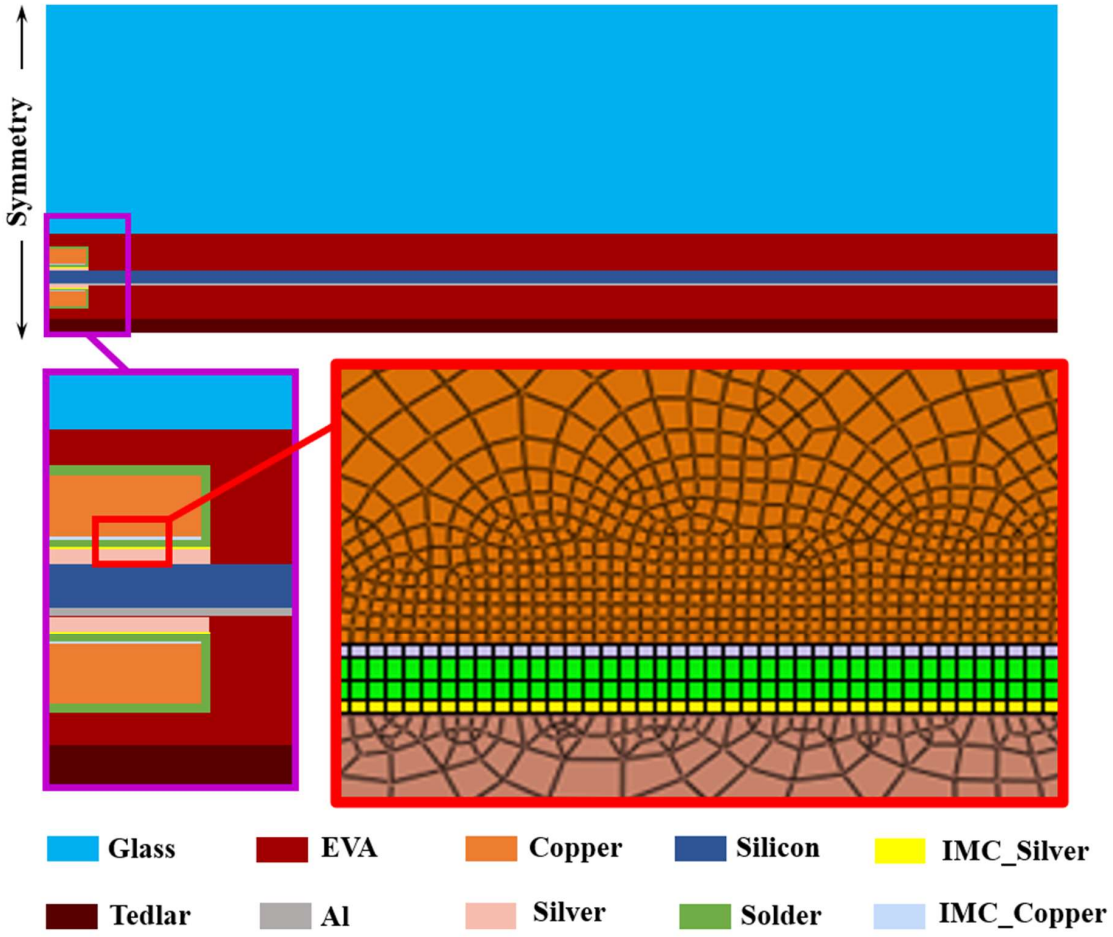

Fig. 1: Schematic view of the simulated conventional PV module interconnection showing the boundary conditions, arrangement of materials and solder joint meshing style.

2.3. Validation of the Methodology

To validate the methodology used for creep-fatigue investigation in this work (including element type, mesh size, and the formulation to estimate the creep-fatigue lifetime), the results of a simulation of SAC solder joint in Wafer Level Chip Scale Packages (WLCSP) were compared with the literature.

Tab. 3 compares the number of cycles to failure (N_f) estimated using the present methodology with the N_f reported in the literatures. There were good agreements between the estimated N_f using the present methodology in this study and the N_f reported from the experiment (9.8% error) as highlighted in Tab.3. Hence, the present practiced methodology to predict the creep-fatigue lifetime of the solder joints can be reasonably used for the lifetime estimation of the creep-fatigue failure in the PV module interconnection solder joints.

Tab. 3: Lifetime model parameters and estimated N_f for the solder joint used in WLCSP.

Lifetime Model Parameters $N_f = C(w_{acc})^{\eta}$	**FEM Simulation** (Lee, Chiang, 2019)	**FEM Simulation** (Tsou, et al., 2017)	**Present FEM Simulation**
w_{acc} (from FEM)	0.35	0.39	0.44
C	145	175	526
η	-2	-1.9	-1
N_f	1152	1058	1112
N_f from experiment (Hsieh, Tzeng, 2014)			
Error for the N_f	13.7%	4.4%	9.8%

3. Results and Discussion

3.1. Creep Behavior of the PV Module Interconnection Solder Joint

The FEM results of the creep stress/strain for each PV module interconnection configuration investigated in this study for 5 thermal cycles are discussed in this section. Fig. 2 shows the equivalent creep strain (CEEQ) distribution in the solder joint of the conventional PV module interconnection with 20µm, 40µm, 200µm and 1000µm in solder, silver, copper thickness and ribbon width, respectively, after 5 thermal cycles (ranging from -40°C to 85°C). The results showed that the maximum CEEQ in the solder joint is located at the side of solder joint, and that the middle of the solder joint experiences minimum CEEQ. The location for the maximum CEEQ found in the solder joint was near to the location of the crack initiation in PV module interconnection solder joint subjected to the high temperature of lamination process found in previous studies (Majd, et al., 2019, 2020a, 2020b, 2022).

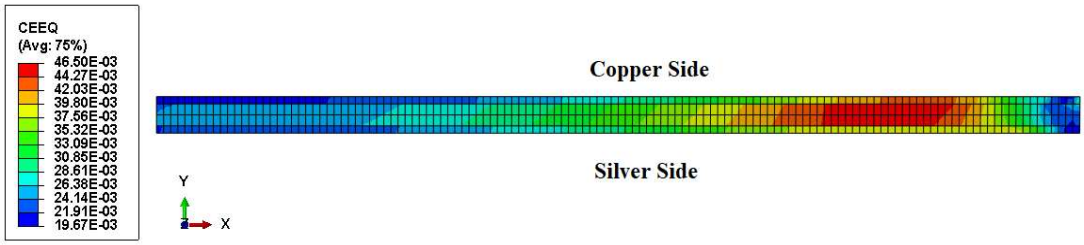

Fig. 2: Equivalent creep strain distribution (CEEQ) in the PV module interconnection solder joint after 5 thermal cycles.

Fig. 3 shows the plot of the hysteresis stress-strain (creep) in shear direction at the element with maximum CEEQ for the solder joint shown in Fig. 2. Fig. 3 suggests that the area enclosed by the stress-strain curve increases marginally with increase in the number of cycles; and this means that the accumulated creep energy in the solder joint increases with thermal cycling which may cause thermal fatigue failure of the solder joint. This increase in the accumulated creep energy is more apparent when using the hysteresis plot of the maximum principle stress via CEEQ for the first 5 thermal cycles, (in Fig. 4) in which the area enclosed by the curve is almost linearly increases by number of cycles.

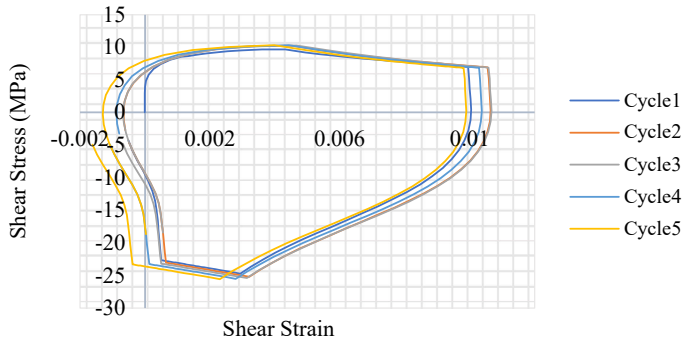

Fig. 3: Plot of the hysteresis shear stress-strain at the element with maximum CEEQ (for 5 thermal cycles).

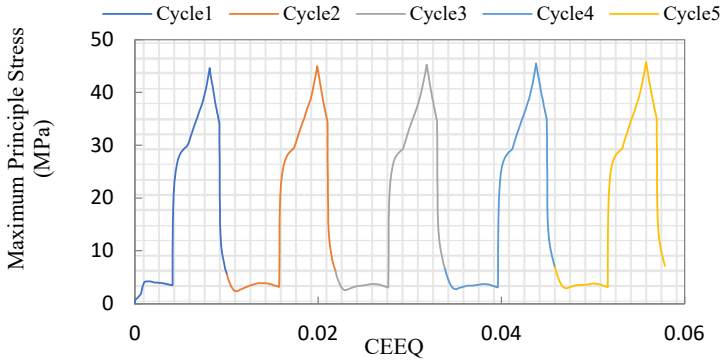

Fig. 4: Plot of the hysteresis maximum principle stress-CEEQ (at the element with maximum CEEQ).

Fig. 5 shows the distribution of the creep-dissipated energy per unit volume for the solder joint shown in Fig. 4, for 5 thermal cycles (ranging from -40°C to 85°C). It can be seen that the distribution of the creep dissipated energy is very similar with the that of the CEEQ (shown in Fig. 2). This indicates that where the CEEQ is maximum, the creep-dissipated energy exhibits the maximum value and vice-versa. Also, the changes in the creep dissipated energy (ECDDEN) at the element with the maximum CEEQ during the first 5 thermal cycles is shown in Fig. 6. As it can be seen in Fig. 5, the side of solder joint exhibits a maximum creep energy and it increases with an increase of the cycle number. This trend is clearly shown in Fig. 6, where by increasing the time (cycle number), the magnitude of the maximum creep dissipated energy increases.

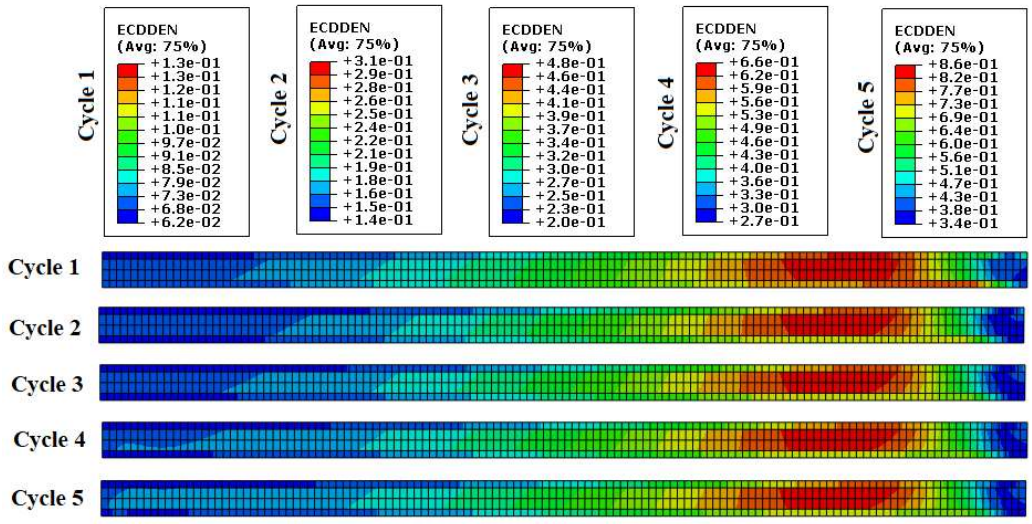

Fig. 5: Distribution of the creep dissipated energy (mJ/mm3) in the solder joints.

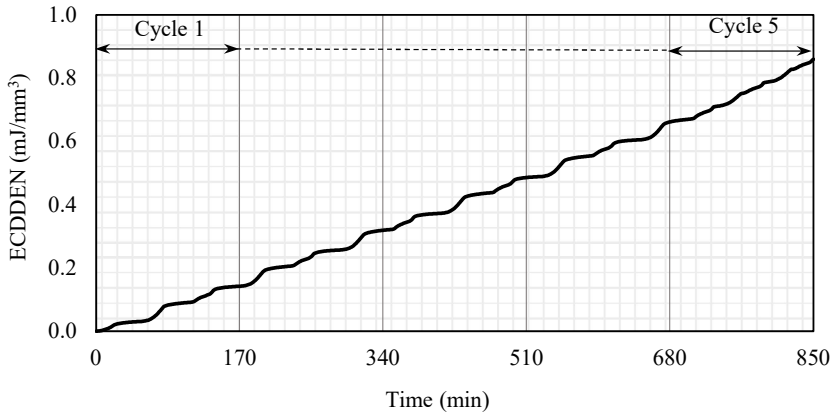

Fig. 6: Creep dissipated energy at the element with maximum CEEQ.

3.2. Fast Cycling Test for Creep-Fatigue Failure Estimation

The empirical models for estimating the creep-fatigue life of SAC (Tin, Silver, Copper) solder alloys joints have been developed by Syed (Syed, 2004). In this approach, he correlated the creep fatigue damage data obtained from laboratory experimental studies with the results of the FEM simulation (i.e. accumulated creep strain and energy density per cycle) to predict thermal creep fatigue life of SAC. His results show that the number of cycles to failure (N_f) for the solder joints under thermal cycling loads are given by the following equation:

$$N_f = (W' w_{acc})^{-1} \qquad \text{(eq. 2)}$$

where W' is the energy density constant for failure (0.0019 for that SAC solder joints) and w_{acc} is the average accumulated creep energy density (per cycle). The average accumulated creep energy density for the solder joints is then given by the following equation:

$$w_{acc} = \frac{\sum W_i V_i}{\sum V_i} \qquad \text{(eq. 3)}$$

where V_i and W_i are the element volume and the accumulated creep energy for each element, respectively.

The Modified Coffin–Manson–Arrhenius lifetime model is one of the most widely used approach for studying the behavior of materials under thermal cycling fatigue; and has been used for predicting the creep life of the solder joints. The solder joint fatigue failure is the mechanical degradation of the solder material due to deformation under cyclic loading and this is known to occur at stress levels below the normal yield stress of solder due to either repeated temperature fluctuations, or mechanical vibrations, or mechanical loads (or combined temperature fluctuations, vibrations and loading). However, in the Coffin-Manson method, the cycling temperature is considered as the main parameter that affects the creep fatigue life. Previous studies have reported on the use of the Modified Coffin-Manson-Arrhenius model for estimating the number of cycles to failure of solder joints for different cycling temperature ranges (Samavatian, et al., 2020; Guyenot, et al., 2011). Held, et al. reported on the creep behavior of the solder joints under fast thermal cycling test and they proposed a descriptive model based on the modified Arrhenius lifetime model for predicting the number of cycles to failure (Nf) for solder joints. The analytical formula that describes the relation between the number of cycles to failure, Nf and cycling temperatures (see equation 4) has been reported by Held, et al. (1997) (Held, et al., 1997).

$$N_f = A * \Delta T^{\alpha} * \exp\left(\frac{Q}{RT_m}\right) \quad \text{(eq.4)}$$

where, Nf *is* the number of cycles to failure, ΔT is the cycling temperature (in Kelvin, R and Q are the gas constant and internal energy, respectively, Tm is the mean cycle temperature (in Kelvin), α is the exponent factor (dependent to the design) and A is a constant for the material.

The exponent factor (α), can be found by rearranging equation 4 for the Field Conditions ($N_{f_{field}}$) and the test conditions ($N_{f_{test}}$), as follows:

$$\frac{N_{f_{field}}}{N_{f_{test}}} = \left(\frac{\Delta T_{field}}{\Delta T_{test}}\right)^{\alpha} * \exp\left(\frac{Q}{R}\left(\frac{1}{T_{m_{field}}} - \frac{1}{T_{m_{test}}}\right)\right) \quad \text{(eq.5)}$$

$$\alpha = \frac{1}{\ln\frac{\Delta T_{field}}{\Delta T_{test}}} \ln\left(\frac{N}{N_{f_{test}} * \exp\left(\frac{Q}{R}\left(\frac{1}{T_{m_{field}}} - \frac{1}{T_{m_{test}}}\right)\right)}\right) \quad \text{(eq.6)}$$

In this study, the exponent factor (α) for the conventional PV module interconnection under any field condition, was found by comparing the correlated FEM results for different temperature intervals (ΔT) with the test condition. Tab. 4 shows the calculated values of accumulated creep energy density per cycle ($wacc$) for different cycling conditions. The values of $wacc$ were calculated (by using equation 3) for the first 5 cycles of each load cycling scenario, and the average is used to estimate the number of cycles to failure (N_f) (see equation

2). Then, using equation 6 gives the value of α based on the comparison of the each field thermal cycling condition with the test thermal cycling condition (temperature ranging from -40°C to 85°C). The results of the study presented in Tab. 4, shows good convergence in the values of $wacc$ for each of the five cycles used for investigating the thermal cycling scenarios; and this provides confirmation that the FEM simulation of the PV module interconnection has been implemented accurately.

To find the generic value of α_m for a given field thermal cycling condition and design, we use the mean value of the calculated α values (see Tab. 4), which was found to be α_m -1.8. This α_m (generic value) found for the conventional PV module interconnection operating under any field thermal cycling condition, can be substituted into equation 4 to determine the number of cycles to failure (N_f) and the associated the creep-fatigue life. This generic value for the exponential factor found in this study can be used for evaluating potential design changes and to facilitate design for reliability validation of different configurations to improve the long-term PV module system reliability.

Tab. 4: Averaged accumulated creep energy density and α for different thermal cycling condition.

T_{min} (°c)	T_{max} (°c)	T_m (k)	ΔT (k)	accumulated creep energy density per cycle (w_{acc})					N_f	α
				w_{acc_1}	w_{acc_2}	w_{acc_3}	w_{acc_4}	$w_{acc_{ave}}$		
-40	**85**	**296**	**125**	**0.157**	**0.158**	**0.158**	**0.158**	**0.158**	**3333**	-
-20	70	298	90	0.088	0.088	0.088	0.088	0.088	5983	-1.93
-10	70	303	80	0.071	0.072	0.072	0.072	0.072	7351	-2.11
-10	60	298	70	0.055	0.055	0.055	0.053	0.055	9530	-1.90
-10	50	293	60	0.042	0.042	0.042	0.040	0.042	12592	-1.74
-10	40	288	50	0.030	0.030	0.030	0.030	0.030	17311	-1.63
-20	60	293	80	0.070	0.070	0.070	0.068	0.070	7271	-1.70
-20	50	288	70	0.055	0.055	0.055	0.055	0.055	9510	-1.54

3.3. Creep-Fatigue Lifetime Estimation

The number of cycles per day used for calculating the creep-fatigue life for PV module operating under thermal cycling has generally been assumed to be l.5 cycles per day (Guyenot, et al., 2011); and this rate 1.5 cycles per day was then used with the calculated number of cycles to failure to determine the numbers of years to failure (Creep-Fatigue lifetime). The effect of different parameters (namely: solder thickness, silver-pad thickness, copper thickness and ribbon width), on the creep-fatigue lifetime of the conventional PV module interconnection (operating under 3 different thermal cycling loads, namely: from temperature ranges of 10°C to 50°C, 0°C to 50°C and 0°C to 60°C) are presented in Fig. 7 to 10. The results showed that for all PV module interconnection dimensions studied, the creep-fatigue lifetime calculated for the thermal cycling loads (namely: the 10°C to 50°C and the 0°C to 50°C) were identical. The results indicate that for all cases studied, the maximum temperature of the cycling load massively impacts the creep-fatigue lifetime; as by increasing the maximum temperature from 50°C to 60°C, the creep-fatigue lifetimes experience 50% decrease. Equally, the results showed that the minimum temperature of the cycling load has much less effect on the creep-fatigue lifetime.

Fig. 7 shows that for solder joints thicker than 20µm, there is no or little change in the creep-fatigue lifetime with increase in the solder joints thickness. The calculated creep-fatigue lifetime of the solder joint of interconnection under thermal cycling in range of 0°C to 50°C (ΔT=50°C) was 26.5 years which is in very good agreement with the reported life (25 years) for similar configuration studied by Guyenot, et al. (2011) (Guyenot, et al., 2011). This provides further validation for the methodology used for this study, as reported in our previous study (Majd, Ekere, 2020a). Fig. 8 shows that the creep-fatigue lifetime increases linearly with increasing silver-pad thickness. For example, increasing the silver-pad thickness from 20µm to 50µm resulted in an increase of about 50% in the creep-fatigue lifetime.

Changing the copper thickness and ribbon width had very marginal effect on the creep-fatigue lifetime (less than 10%) as highlighted by Fig. 9 and Fig. 10. However, for reducing the electrical resistance in the ribbon, the ribbon should be designed to provide enough cross section of ribbon (at least 0.15mm^2). Hence, the

minimum acceptable copper thickness is considered as 150µm when the ribbon width is no less than 1mm. Alternatively, for the ribbons width with less than 1mm (e.g. 900µm), the copper with thickness higher than 150µm should be used. Our results shows that the ribbon with ribbon width of 900µm and copper thickness of 175µm has about 1% less creep-fatigue life compared to the ribbon with 1mm width, and 150µm copper thickness.

In summary, the methodology developed for this study to investigate the effect of the four geometrical parameters on the creep-fatigue lifetime of conventional PV module interconnection provided the results for determining the optimal design for long-term reliability. Our results recommend the 20µm solder thickness, 40µm-50µm silver-pad thickness, 150µm copper thickness and 1mm ribbon width geometry.

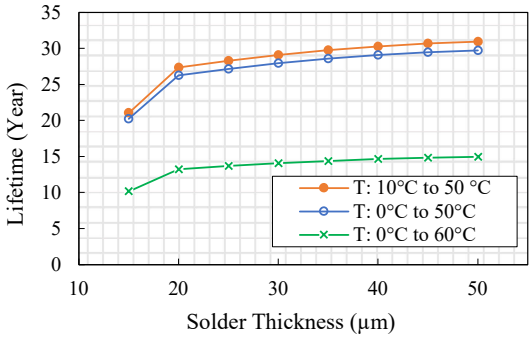

Fig. 7: Effect of solder thickness on the creep-fatigue lifetime of the conventional PV module interconnection operating under 3 different thermal cycling conditions.

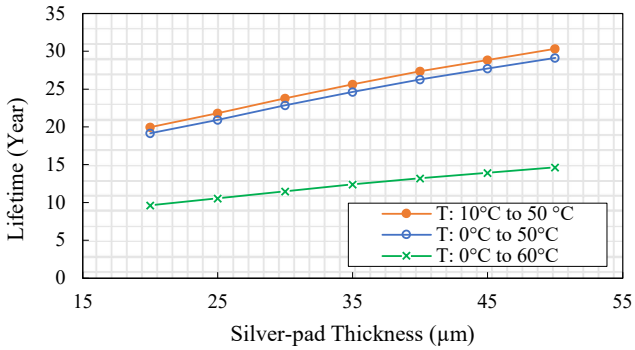

Fig. 8: Effect of silver-pad thickness on the creep-fatigue lifetime of the conventional PV module interconnection.

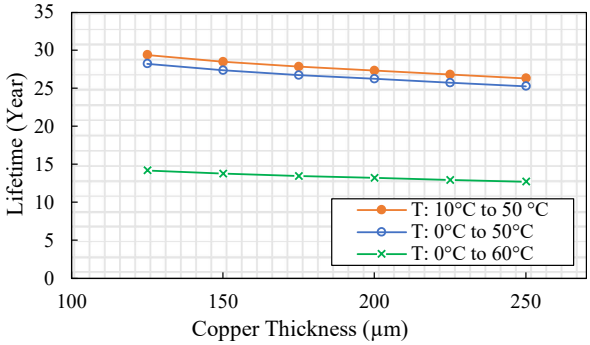

Fig. 9: Effect of copper thickness on the creep-fatigue lifetime of the conventional PV module interconnection.

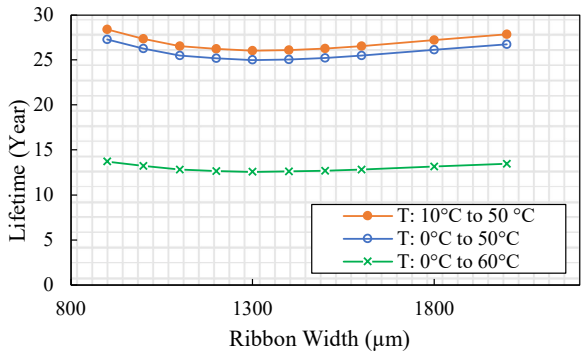

Fig. 10: Effect of ribbon width on the creep-fatigue lifetime of the conventional PV module interconnection.

4. Conclusion

The strain and stress induced by the field thermal cycling loads leads to the creep-fatigue failure mode of the solder joint which adversely affect the reliability of the PV module. An attempt has been made to investigate the creep behavior of the solder joints for the conventional PV module interconnection with different dimensions using the FEM simulation in ABAQUS software. Our results showed that the maximum shear creep strain in the solder joint was located at the corner of the connection area in copper side; and that this location exhibited the highest propensity for creep fatigue failure during the operation. In the study, the total dissipated energy was used to find the number of cycles to failure for each of the PV module interconnections operating under the test and field thermal cycling load. The exponent factor of Coffin–Manson–Arrhenius approach for determining the Creep-Fatigue life of the PV module interconnections was determined to be -1.8; and this generic exponent factor value was then used to determine the solder joint's creep-fatigue life under thermal cycling operating conditions. It was found that, for all cases studied, the maximum temperature of the cycling load massively impacts the creep-fatigue lifetime with a 50% decrease in creep-fatigue lifetimes when the maximum temperature was increased from 50°C to 60°C. On the other hand, the minimum temperature of the cycling load showed much less effect on the creep-fatigue lifetime. There was little or no change in the creep-fatigue lifetime with increase in the solder joints thickness for solder joints thicker than 20µm. similarly, changing the copper thickness and ribbon width had very marginal effect on the creep-fatigue lifetime (≤ 10%) whereas the creep-fatigue lifetime increases linearly with increasing silver-pad thickness. Our results recommend the 20µm solder thickness, 40µm-50µm silver-pad thickness, 150µm copper thickness and 1mm ribbon width geometry. The presented results of the PV module interconnections study can be used to evaluate potential design changes and facilitate the design for reliability validation of different configurations for improving the long-term PV module system reliability.

5. Acknowledgment

The authors would like to acknowledge the support of the Faculty of Science and Engineering, University of Wolverhampton for providing the sponsorship to Dr. Alireza Eslami Majd's Ph.D. study. This work was also partially supported by the INNOVATE UK project No: 833831.

6. References

Akay, H.U., Liu, Y., Rassaian, M., 2003. Simplification of finite element models for thermal fatigue life prediction of PBGA packages. Journal of Electronic Packaging, Transactions of the ASME. 125 (3), 347–353. DOI:10.1115/1.1569956

Amalu, E.H., Ekere, N.N., 2016. Modelling evaluation of Garofalo-Arrhenius creep relation for lead-free solder joints in surface mount electronic component assemblies. Journal of Manufacturing Systems. 39, 9–23. doi.org/10.1016/j.jmsy.2016.01.002

Andersson, C., Sun, P., Liu, J., 2006. Low cycle fatigue of Sn-based lead-free solder joints and the analysis of fatigue life prediction uncertainty. Proceedings of the eight IEEE CPMT International Symposium on High Density Packaging and Component Failure Anlaysis (HDP´06), Shanghai, 09 October. 272–279. DOI: 10.1109/HDP.2006.1707606

Baber, F., and Guven, I., 2017. Solder joint fatigue life prediction using peridynamic approach.

Microelectronics Reliability. 79, 20–31. doi.org/10.1016/j.microrel.2017.10.004

Che, F.X., and Pang, J.H.L., 2004. Thermal fatigue reliability analysis for PBGA with Sn-3.8 Ag-0.7 Cu solder joints. Proceedings of 6th Electronics Packaging Technology Conference (EPTC 2004). (IEEE Cat. No. 04EX971), Singapore, 08-10 December. 787–792. DOI: 10.1109/EPTC.2004.1396715.

Chen, Y., Jin, Y., and Kang, R., 2017. Coupling damage and reliability modeling for creep and fatigue of solder joint. Microelectronics Reliability. 75, 233–238. doi.org/10.1016/j.microrel.2017.03.016

Chen, Z., Zhang, Z., Dong, F., Liu, S., and Liu, L., 2021. A Hybrid Finite Element Modeling: Artificial Neural Network Approach for Predicting Solder Joint Fatigue Life in Wafer-Level Chip Scale Packages. Journal of Electronic Packaging.143 (1). doi.org/10.1115/1.4047227

Cho, Y., Jang, J., and Jang, G., 2018. Sensitivity analysis on the fatigue life of solid state drive solder joints by the finite element method and Monte Carlo simulation. Microsystem Technologies. 24 (11), 4669–4676. doi.org/10.1007/s00542-018-3819-0

Darveaux, R., 2002. Effect of simulation methodology on solder joint crack growth correlation and fatigue life prediction. Proceedings of 50th Electronic Components and Technology Conference (Cat. No.00CH37070), Las Vegas, 21-24 May. 124 (3), 147–154. DOI: 10.1109/ECTC.2000.853299

Depiver, J. a, Mallik, S., and Harmanto, D., 2021. Solder joint failures under thermo-mechanical loading conditions–A review. Advances in Materials and Processing Technologies. 7 (1), 1–26. doi.org/10.1080/2374068X.2020.1751514

Majd, A., and Ekere, N.N., 2019. Numerical analysis on thermal crack initiation due to non-homogeneous solder coating on the round strip interconnection of photo-voltaic modules. Solar Energy. 194, 649-655. doi.org/10.1016/j.solener.2019.10.092

Majd, A., Ekere, N.N., 2020. Study of High Temperature Crack Initiation and Growth in Light Capturing Ribbon (LCR) PV Module Interconnection. Advanced Materials Science and Technology. 2(2). doi.org/10.37155/2717-526X-0202-3

Majd, A., Ekere, N.N., 2020. Crack initiation and growth in PV module interconnection. Solar Energy. 206, 499-507. doi.org/10.1016/j.solener.2020.06.036

Majd, A., Ekere, N.N., Darvazi, A.R., Sedehi, A.A., 2022. Creep- Fatigue Lifetime Estimation of Efficient Photovoltaic Module Ribbon Interconnection. Microelectronics Reliability. 139, 114831. doi.org/10.1016/j.microrel.2022.114831

Guyenot, M., Peter, E., Zerrer, P., Kraemer, F., and Wiese, S., 2011. Enhancing the lifetime prediction methodology for photovoltaic modules based on electronic packaging experience. 12th Intl. Conf. on Thermal, Mechanical & Multi-Physics Simulation and Experiments in Microelectronics and Microsystems, Linz, 18-20 April. 1–4. DOI: 10.1109/ESIME.2011.5765781

Halouani, A., Cherouat, A., Miladi Chaabane, M., Haddar, M., 2020. Modeling and experimental investigation of damage initiation and propagation of LQFP package under thermal cycle. Microsystem Technologies. 26, 3011–3021. doi.org/10.1007/s00542-020-04884-9

Han, C., Han, B., 2014. Board level reliability analysis of chip resistor assemblies under thermal cycling: A comparison study between SnPb and SnAgCu. Journal of Mechanical Science and Technology. 28 (3), 879–886. doi.org/10.1007/s12206-013-1154-z8

Held, M., Jacob, P., Nicoletti, G., Scacco, P., Poech, M.-H., 1997. Fast power cycling test of IGBT modules in traction application. Proceedings of second international conference on power electronics and drive systems, Singapore, 26-29 May. 1, 425–430. DOI: 10.1109/PEDS.1997.618742

Hsieh, M., Tzeng, S., 2014. Solder joint fatigue life prediction in large size and low cost wafer-level chip scale packages. 15th International Conference on Electronic Packaging Technology, Chengdu, 12-15 August. 496–501. DOI: 10.1109/ICEPT.2014.6922704

Hund, T.D., Burchett, S.N., 1991. Solder fatigue reduction in point focus photovoltaic concentrator modules. Proceedings of The Conference Record of the Twenty-Second IEEE Photovoltaic Specialists Conference, Las Vegas, 07-11 October. DOI: 10.1109/PVSC.1991.169310

IEA, 2020. Solar PV - Analysis - IEA.

International Electrotechnical Commission, 2016. IEC 61215-2: Terrestrial Photovoltaic (PV) Modules – Design Qualification and Type Approval -Part 2: Test procedures.

IRENA, 2019. Future of solar photovoltaic: Deployment, investment, technology, grid integration and socio-economic aspects (A Global Energy Transformation: paper).

Itoh, U., Yoshida, M., Tokuhisa, H., Takeuchi, K., Takemura, Y., 2014. Solder joint failure modes in the conventional crystalline Si module. Energy Procedia, 55, 464–468. doi.org/10.1016/j.egypro.2014.08.010

Knecht, S., Fox, L.R., 1990. Constitutive relation and creep-fatigue life model for eutectic tin-lead solder. IEEE Transactions on Components, Hybrids, and Manufacturing Technology. 13 (2), 424–433. DOI: 10.1109/33.56179

Lee, W.W., Nguyen, L.T., Selvaduray, G.S., 2000. Solder joint fatigue models: review and applicability to chip scale packages. Microelectronics reliability. 40 (2), 231–244. doi.org/10.1016/S0026-2714(99)00061-X

Lee, Y.C., Chiang, K.N., 2019. Reliability Assessment of WLCSP using Energy Based Model with Inelastic Strain Energy Density. Proceedings of International Conference on Electronics Packaging (ICEP), Niigata, 17-20 April. 329–332. DOI: 10.23919/ICEP.2019.8733436

Li, X., Sun, R., Wang, Y., 2017. A review of typical thermal fatigue failure models for solder joints of electronic components. Proceedings of IOP Conference Series: Materials Science and Engineering, 3rd International Conference on Applied Materials and Manufacturing Technology (ICAMMT 2017), Changsha, 23–25 June. 242 (1). DOI:10.1088/1757-899X/242/1/012103

Ma, H., 2009. Constitutive models of creep for lead-free solders. Journal of Materials Science. 44 (14), 3841–3851. doi.org/10.1007/s10853-009-3521-9

Ogbomo, O.O., Amalu, E.H., Ekere, N.N., Olagbegi, P.O., 2018. Effect of operating temperature on degradation of solder joints in crystalline silicon photovoltaic modules for improved reliability in hot climates. Solar Energy. 170, 682–693. doi.org/10.1016/j.solener.2018.06.007

Samavatian, V., Iman-Eini, H., Avenas, Y., Samavatian, M., 2020. Effects of creep failure mechanisms on thermomechanical reliability of solder joints in power semiconductors. IEEE Transactions on Power Electronics. 35 (9), 8956–8964. DOI: 10.1109/TPEL.2020.2973312

Schubert, A., Dudek, R., Auerswald, E., Gollhardt, A., Michel, B., Reichl, H., 2003. Fatigue life models for SnAgCu and SnPb solder joints evaluated by experiments and simulation. Proceedings of 53rd Electronic components and technology conference. New Orleans, 27-30 May. 603–610. DOI: 10.1109/ECTC.2003.1216343

Steinhorst, P., Poller, T., Lutz, J., 2013. Approach of a physically based lifetime model for solder layers in power modules. Microelectronics Reliability. 53 (9–11), 1199–1202. doi.org/10.1016/j.microrel.2013.07.094

Syed, A., 2004. Accumulated creep strain and energy density based thermal fatigue life prediction models for SnAgCu solder joints. Proceedings of 54th electronic components and technology conference. (IEEE Cat. No. 04CH37546), Las Vegas, 04-04 June. 1, 737–746. DOI: 10.1109/ECTC.2004.1319419

Tsou, C.Y., Chang, T.N., Wu, K.C., Wu, P.L., Chiang, K.N., 2017. Reliability assessment using modified energy based model for WLCSP solder joints. Proceedings of International Conference on Electronics Packaging (ICEP), Yamagata, 19-22 April. 7–15. DOI: 10.23919/ICEP.2017.7939312

Yao, Y., Long, X., Keer, L.M., 2017. A review of recent research on the mechanical behavior of lead-free solders. Applied Mechanics Reviews. 69 (4). doi.org/10.1115/1.4037462

Zhang, X.P., Yin, L.M., Yu, C.B., 2008. Thermal creep and fracture behaviors of the lead-free Sn–Ag–Cu–Bi solder interconnections under different stress levels. Journal of materials science: materials in electronics. 19 (4), 393–398. doi.org/10.1007/s10854-007-9351-0

Zhu, Y., Li, X., Gao, R., Wang, C., 2014. Low-cycle fatigue failure behavior and life evaluation of lead-free solder joint under high temperature. Microelectronics Reliability. 54 (12), 2922–2928. doi.org/10.1016/j.microrel.2014.08.016